Proceedings of ASME/STLE International Joint Tribology Conference
IJTC2007
October 22-24, 2007, San Diego, California USA

IJTC2007-44280

TEMPERATURE DISTRIBUTION OF A WAVE JOURNAL BEARING. COMPARISON WITH TEST DATA

Nicoleta M. Ene
MIME Department
The University of Toledo, Toledo, Ohio

Florin Dimofte
The University of Toledo
at NASA Glenn Research Center, Cleveland, Ohio

Theo G. Keith, Jr.
MIME Department
The University of Toledo, Toledo, Ohio

Robert F. Handschuh
US Army Research Laboratory
at NASA Glenn Research Center, Cleveland, Ohio

ABSTRACT

An advanced three-dimensional model is developed to compute the temperature distribution in a wave journal bearing. The analysis takes into account the heat transfer between the film and both the shaft and the bush. The theoretical results are validated by comparison with experimental data.

INTRODUCTION

When rotating at high speeds, journal bearings frequently experience high temperature gradients in the fluid film. Therefore, in order to accurately predict the bearing performance parameters, a thermohydrodynamic (THD) analysis that accounts for heat dissipation is generally required ([1], [4]). This paper presents a three dimensional THD model which is used to predict the temperature distribution in a three wave journal bearing. The theoretical results are compared to experimental data obtained at the NASA Glenn Research Center.

NOMENCLATURE

e = eccentricity, [m]
e_w = wave amplitude [m]
h = film thickness [m]
l = length of the bearing [m]
n_w = number of the waves
p = pressure [Pa]
u, v, w =velocity components [m/s]
z = axial coordinate [m]
C = clearance [m]
R = shaft radius [m]
T_s = supply temperature [°C]
W = load capacity [N]
T = fluid temperature [°C]
T_0 = initial temperature [°C]
β = bulk modulus, Pa
μ = dynamic viscosity, Ns/m^2
ρ = density, kg/m^3
θ = angular coordinate [rad]
ω = angular speed [rad/s]
Subscripts
r = rotor s = supply
b = bush
Over-bar = nondimensional parameters

THE WAVE BEARING CONCEPT

The wave bearing is an alternative to the circular journal bearing ([2], [3]). Unlike the plain journal bearing, the wave bearing has a slight but precise variation of its profile geometry. The variation is such that a wave profile is circumscribed on the inner bearing diameter. The wave amplitude is typically a fraction of the radial clearance (0.05-0.6).

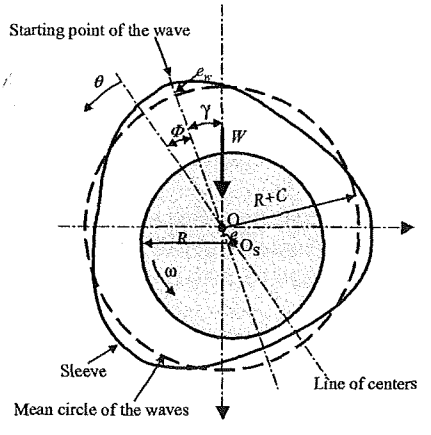

Fig. 1 The Geometry of a Three-Wave Journal Bearing

A wave bearing can have two or more waves. A three-wave bearing is represented in Fig. 1. In order to visualize the wave-bearing concept, in Fig. 1, the amplitude of the wave is greatly

exaggerated. The radial clearance, C, is the difference between the radius of the mean circle of the waves and the shaft radius, R. The clearance is usually less than one thousandth of the journal radius.

The load capacity W of the film is due to the rotation of the shaft and to the variation of the fluid film thickness along the circumference. From geometrical considerations, it can be shown that the fluid film thickness is given by:

$$h = C + e\cos(\theta) + e_w \cos\left[n_w(\theta + \Phi)\right] \tag{1}$$

Numerical and experimental results show that the three-wave bearing has the best performance. The three-wave bearing has improved stability characteristics and enhanced stiffness compared to a circular journal bearing having the same geometrical characteristics.

BASIC EQUATIONS

The pressure distribution is determined by integrating the nondimensional generalized Reynolds equation for an incompressible fluid under steady loading conditions:

$$\frac{\partial}{\partial\theta}\left(\bar{h}^3 g\bar{G}\bar{\beta}\frac{\partial\alpha}{\partial\theta}\right) + \frac{\partial}{\partial\bar{z}}\left(\bar{h}^3 g\bar{G}\bar{\beta}\frac{\partial\alpha}{\partial\bar{z}}\right) = \frac{\partial}{\partial\theta}\left(\bar{h} - \bar{h}\frac{\bar{I}_2}{\bar{J}_2}\right) \tag{2}$$

where:

$$\bar{G} = \int_0^1 \frac{\bar{y}}{\bar{\mu}}\left(\bar{y} - \frac{\bar{I}_2}{\bar{J}_2}\right)d\bar{y} \qquad \bar{I}_2 = \int_0^1 \frac{\bar{y}}{\bar{\mu}}d\bar{y}$$

$$\bar{J}_2 = \int_0^1 \frac{1}{\bar{\mu}}d\bar{y} \qquad \bar{\beta} = \frac{\beta}{\mu_0\omega}\left(\frac{C}{R}\right)^2$$

In this equation, α is the variable introduced by Elrod in order to take in account the rupture and reformation of the fluid film. It has two different interpretations: the non dimensional density in the full film and the fractional film content in the cavitation region. The axial ends of the bearing are assumed to be exposed to atmospheric pressure. The pressure in the region of the supply pockets is assumed to be equal to the supply pressure.

For the lubricant used in experiments, a double exponential law is suitable to describe the variation of effective viscosity with temperature:

$$\upsilon = e^{\log\upsilon_0 e^{-\alpha_\upsilon(T-T_0)}} \tag{3}$$

where υ_0 is the kinematic viscosity of the fluid corresponding to the temperature T_0. The coefficient α_υ is calculated knowing the value of viscosity corresponding to another temperature.

The dependency of the lubricant density, thermal conductivity and specific heat with the temperature are also considered.

The temperature distribution in the fluid film is determined by solving the energy equation:

$$P_e\left[\bar{u}\left(\frac{\partial\bar{T}}{\partial\theta} - \frac{\bar{y}}{\bar{h}}\frac{d\bar{h}}{d\theta}\frac{\partial\bar{T}}{\partial\bar{y}}\right) + \frac{\bar{v}}{\bar{h}}\frac{\partial\bar{T}}{\partial\bar{y}} + \eta\bar{w}\frac{\partial\bar{T}}{\partial\bar{z}}\right] = \frac{1}{\bar{h}^2}\frac{\partial^2\bar{T}}{\partial\bar{y}^2} + N_d\frac{\bar{\mu}}{\bar{h}^2}\left[\left(\frac{\partial\bar{u}}{\partial\bar{y}}\right)^2 + \left(\frac{\partial\bar{w}}{\partial\bar{y}}\right)^2\right] \tag{4}$$

where:

$$P_e = \frac{\rho C_p\omega C^2}{K_f} \text{ and } N_d = \frac{\mu_0\omega^2R^2}{K_fT_0}$$

are the Peclet number and the dissipation number, respectively.

The temperature field in the sleeve is described by the Laplace equation:

$$\frac{\partial^2\bar{T}_b}{\partial\bar{r}^2} + \frac{1}{\bar{r}}\frac{\partial\bar{T}_b}{\partial\bar{r}} + \frac{1}{\bar{r}^2}\frac{\partial^2\bar{T}_b}{\partial\theta^2} + \eta^2\frac{\partial^2\bar{T}_b}{\partial\bar{z}^2} = 0 \tag{5}$$

where

$$\bar{r} = \frac{r}{R},\ \bar{T}_b = \frac{T_b}{T_0}.$$

Because the shaft is rotating with great rotational speeds, its temperature is independent of the angular coordinate θ. Consequently, the conduction equation for the shaft is reduced to:

$$\frac{\partial^2\bar{T}_r}{\partial\bar{r}^2} + \frac{1}{\bar{r}}\frac{\partial\bar{T}_r}{\partial\bar{r}} + \eta^2\frac{\partial^2\bar{T}_r}{\partial\bar{z}^2} = 0 \tag{6}$$

where:

$$\bar{r} = \frac{r}{R},\ \bar{T}_r = \frac{T_r}{T_0}.$$

At the oil / sleeve and oil / shaft interfaces, the continuity of the heat fluxes are considered. On the external surfaces of the sleeve and of the shaft, free convection is assumed. At inlet zones, the mixture temperature is determined using the flow and heat conservation equations.

The generalized Reynolds equation, Eq. (2), and the Laplace equations, Eqs. (5) and (6), are solved using finite difference and over-relaxation successive methods. The parabolic energy equation in the film is solved using an implicit finite difference method combined with a Richtmyer technique, when a reverse flow occurs.

DESCRIPTION OF TEST RIG

Figure 2 shows a 3D cross section of the test rig. The rig shaft is supported by two end bearings. There are two test bearings installed in the load ring. The load ring is connected to the loading system. The position of the shaft with respect to the test bearing sleeves is indicated by the proximity probes located on both sides of the load ring. Thermocouples are installed in the metal of the test bearing sleeves, in the supply pockets, and in the oil input and output passage to and from the test bearings. Measurements were performed at a shaft speed of 8,000 RPM and total loads to 20,000 N. Results were recorded by an Escort Data Acquisition System.

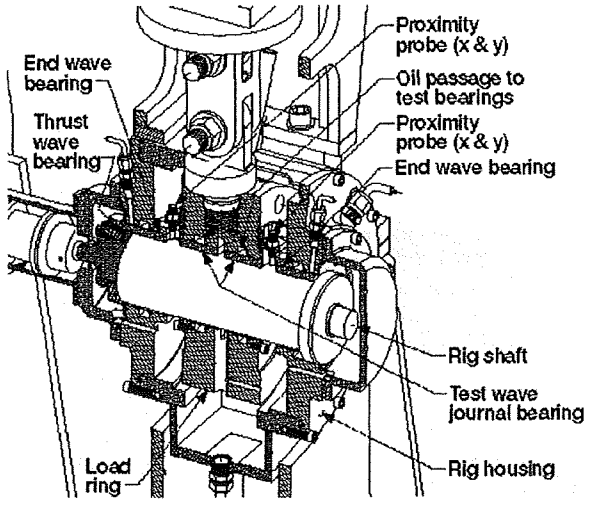

Fig. 2 A 3D cross section of the test rig

RESULTS

The main characteristics of the test wave bearing are presented in Table 1. The bearing has three axial supply grooves which are situated near the points where the amplitude of the wave is maximum.

Table 1 Main Characteristics of the Test Bearing

Bearing radius	R [mm]	34
Bearing length	L [mm]	38
Sleeve outer radius	R_s [mm]	39
Radial clearance	C [μm]	37
Wave amplitude	e_w [μm]]	6
Supply groove axial length	l_p [mm]	30
Supply groove width	b [mm]	5
Lubricant	Mil-L-23699	

The circumferential temperature distributions at film – sleeve interface in the mid section of the bearing for two different conditions are presented in Figs. 3 and 4. The theoretical results are generally in good agreement with the experiment. The largest disagreement between theory and experiment occurs close to the axial groove which is situated in the cavitation zone.

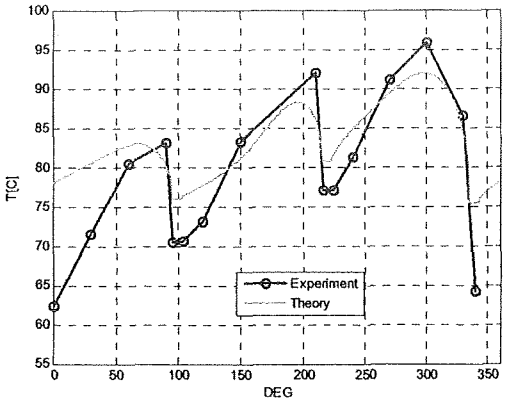

Fig. 3 Circumferential temperature distribution in the film - bush interface (W=4506 N, ω=7991 RPM, p_s=0.53 MPa, T_s=51.94 °C)

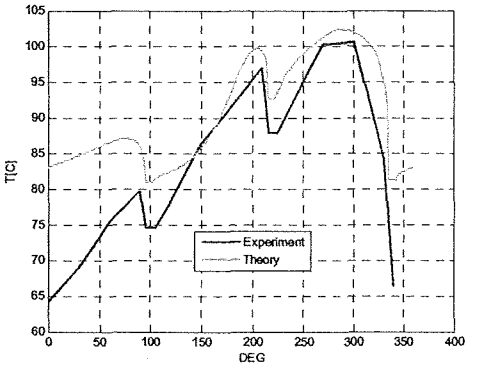

Fig. 4 Circumferential temperature distribution in the film - bush interface (W=8807 N, ω=8016 RPM, p_s=0.48 MPa, T_s=57.2 °C)

REFERENCES

[1] Bouyer, J. and Fillon, M., 2003, "Improvement of the THD Performance of a Misaligned Plain Journal Bearing", *Trans. of ASME*, **125**, pp. 334-342

[2] Dimofte, F. 1995, "Wave Journal Bearing with Compressible Lubricant – Part I: The Wave Bearing Concept and a Comparison to the Plain Circular Bearing", *STLE Trib. Trans.*, **38**, 1, pp. 153-160

[3] Dimofte, F. 1995, "Wave Journal Bearing with Compressible Lubricant – Part II: A Comparison of the Wave Bearing with a Groove Bearing and a Lobe Bearing", *STLE Trib. Trans*, **38**, 2, pp. 364-372

[4] Ferron, J, Frêne, J. and Boncompain, R., 1983, "A Study of the Thermohydrodynamic Performance of a Plain Journal Bearing Comparison Between Theory and Experiments", *Trans. of ASME*, **105**, pp. 422-428